Heat Stress Monitoring in Construction for Risk-Informed Decision-Making

Yoojun Kim[1] and Youngjib Ham, Ph.D., A.M.ASCE[2]

[1]Ph.D. Student, Dept. of Construction Science, Texas A&M Univ., TX.
Email: yoojun@tamu.edu
[2]History Maker Homes Endowed Associate Professor, Dept. of Construction Science, Texas A&M Univ., TX. Email: yham@tamu.edu

ABSTRACT

Heat-related hazards present significant challenges in construction. To effectively mitigate these safety risks, timely assessment of heat stress is vital for implementing heat mitigation strategies. Current field measurement approaches, however, encounter temporal and spatial limitations in monitoring heat stress. This study proposes a framework for near-real-time analysis of spatial heat hazards at construction sites. The framework incorporates 3D modeling to address geometric features and a customized weather station to monitor meteorological conditions. The collected meteorological data is transmitted to a server computer, where heat risks are simulated based on the geometric and meteorological conditions in construction sites. Additionally, the study presents preliminary results comparing the accuracy of this simulation-based approach to on-site measurements using a black globe thermometer and net radiometers. The proposed framework is expected to enhance our understanding of heat risks and enable more effective implementation of protective measures in time-sensitive situations relevant to heat risk.

INTRODUCTION

Extreme heat is the leading cause of weather-related fatalities in the United States (Jones et al. 2021). Climate change exacerbates these threats to public and occupational health, particularly for workers in climate-sensitive occupations, such as construction workers (Gao et al. 2018). These workers face heightened vulnerability to heat-related safety hazards due to direct exposure to outdoor thermal environments during work hours (Lin and Chan 2009). To mitigate the adverse effects of heat in the workplace, it is crucial to identify areas with pronounced hazards and understand the underlying factors contributing to them. This understanding enables risk-informed decision-making for implementing preventive measures, such as frequent breaks, resting in shaded areas, and rehydration. Accordingly, National Institute for Occupational Safety & Health (NIOSH) recommends measuring the heat-related meteorological conditions in work areas at least one-hour intervals during the hottest months (Jacklitsch et al. 2016).

Despite the accumulating evidence indicating that the increased heat-related hazards have emerged as a major concern in construction (Dong et al. 2019; Orlov et al. 2019), it remains difficult to assess the temporal and spatial aspects of heat risks impacting the health and safety of construction workers. Previous studies have evaluated thermal conditions at specific locations using on-site measurements with black globe thermometers (Chan et al. 2012; Fang et al. 2021; Wong et al. 2014; Yi et al. 2016). Although this method provides valuable insights into instantaneous heat radiation levels at selected locations, it has inherent limitations in terms of both temporal and spatial coverage. For example, the black globe thermometer, originally designed for indoor applications, often requires additional calibration to improve its accuracy, and exhibits a slow response time due to delayed heat transfer from the globe (Tang and Li 2022). Furthermore, this on-site measurement method encounters difficulties in addressing spatial variations, as acquiring multiple simultaneous measurements across site areas is challenging. The dynamic nature of construction environments further complicates the implementation of this method, requiring frequent adjustments to measurements.

To address this knowledge gap, this study introduces a framework for near-real-time analysis of spatial heat hazards at construction sites. Complementing the spatial limitations of on-site measurement approaches, this framework integrates site geometric modeling and a simulation-based heat risk assessment, offering a comprehensive assessment of spatio-temporal heat hazards affecting construction workers. Furthermore, the study presents preliminary results on the accuracy of the simulation-based approach compared to on-site measurements using a black globe thermometer and net radiometers. This framework is expected to benefit practitioners with near-real-time insights, facilitating prompt decisions to prevent heat-related accidents in construction settings. Utilizing the WBGT index, it generates heat risk maps in near-real-time, highlighting areas of significant concern. These maps, grounded in the values of the WBGT index, can be integrated with established heat mitigation guidelines, establishing this framework as a promising tool for safeguarding the health and safety of construction workers.

SITE-SCALE HEAT RISK MONITORING

The proposed framework comprises three main steps: (1) meteorological and geometric data capture, (2) site-scale heat risk assessment, and (3) risk-informed decision-making, as illustrated in Figure 1. In the first step, a geometric model of the site is generated by UAV photogrammetry. In addition, meteorological data are obtained through a customized weather station deployed on-site and subsequently transmitted to a server for analysis. Next, a microclimate simulation is performed to assess heat-related risks throughout the construction site. Ultimately, the framework facilitates risk-informed decision-making by complying with established heat safety guidelines.

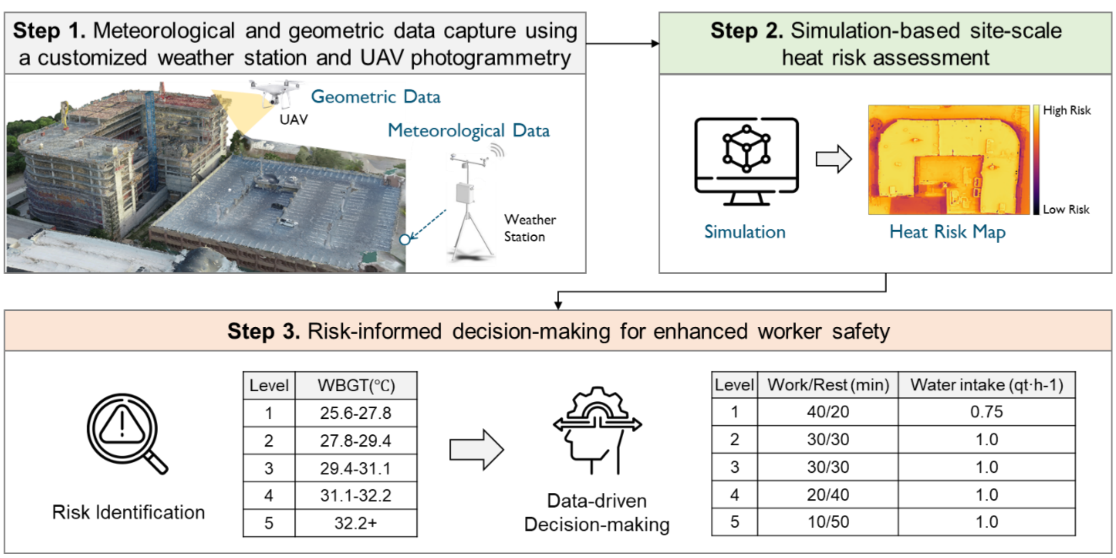

Figure 1. Overview of the proposed framework.

METEOROLOGICAL AND GEOMETRIC DATA CAPTURE

Our research team has developed a customized weather station to monitor on-site meteorological conditions associated with occupational heat hazards, as depicted in Figure 2. The station consists of multiple components, including a digital sensor for air temperature (T_a) and relative humidity (RH) measurements, a wind sentry anemometer for air velocity (V_a) measurement, and a sunshine pyranometer for quantifying global horizontal irradiance (GHI). By leveraging a cellular module, the station enables near-real-time data transmission to a server computer. Additionally, the collected data is stored in two separate locations: an internal data logger and an external SD card.

#	Type	Variable(s) or function(s)
1	Sensor	Air temperature
		Relative humidity
2	Sensor	Global horizontal irradiance
3	Sensor	Air velocity
4	Data logger	Data storage
5	Cellular module	Communication
6	Regulator	Charging regulator
7	Power supply	Power

Figure 2. Configurations of the customized weather station.

The proposed framework leverages UAV photogrammetry to generate a site geometric model. UAV photogrammetry has been widely employed in various construction applications, such as progress monitoring (Reja et al. 2022) and disaster risk assessment (Kamari and Ham 2022). Building upon the UAV photogrammetry, a digital surface model (DSM) is created to provide a detailed representation of topographic information on surfaces, including the elevations of built environments. This DSM delivers crucial site geometric information for estimating shade patterns, sky view factors, and ground view factors in microclimate simulations. To enhance computational efficiency, the spatial resolution of DSM is resampled to 0.5 meters, with each pixel representing the average height within a 0.25 square meter area. Figure 3 illustrates the process of geometric data capture through UAV photogrammetry. Additionally, a surface material map is registered based on the resampled DSM to account for the thermophysical properties of surface materials, which predominantly affect longwave radiation fluxes.

SIMULATION-BASED SITE-SCALE HEAT RISK ASSESSMENT

The site-scale risk assessment process consists of two main steps: (1) microclimate simulation, and (2) heat risk assessment based on Wet Bulb Globe Temperature (WBGT). The process begins with a microclimate simulation, which accounts for both geometric features and meteorological conditions. In the proposed framework, the simulation mechanisms are grounded in the Solar and LongWave Environmental Irradiance Geometry (SOLWEIG) model which has been widely acknowledged and validated in prior studies (Jänicke et al. 2015; Kántor et al. 2018). The model calculates shortwave-induced radiant flux by considering solar irradiance and site geometry, impacting shading effects. Additionally, the model computes longwave-induced radiant flux by incorporating the thermophysical properties of surface materials. More details on the SOLWEIG model can be found in (Lindberg and Grimmond 2011; Lindberg et al. 2016). The simulation generates a spatially-varying mean radiant temperature (T_{mrt}) map for construction sites. Subsequently, the heat risk at construction sites is assessed based on WBGT, a thermo-physiological model for determining environmental heat hazards recommended by NIOSH (Jacklitsch et al. 2016). Equation (1) is used for calculating WBGT in outdoor settings.

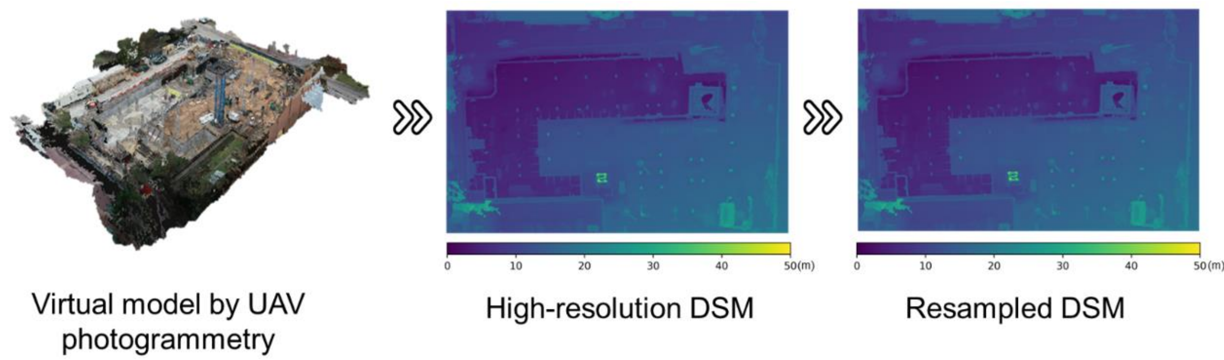

Figure 3. Process of geometric data capture through UAV photogrammetry.

$$\mathrm{WBGT} = 0.7\mathrm{T_w} + 0.2\mathrm{T_g} + 0.1\mathrm{T_a} \tag{1}$$

Where T_w is the web-bulb temperature and T_g is the globe temperature. T_w is determined using the empirical Equation (2) suggested by (Stull 2011), which takes into account T_a and RH:

$$\mathrm{T_w} = \mathrm{T_a} \arctan[0.151977(\mathrm{RH} + 8.313659)^{0.5}] + \arctan(\mathrm{T_a} + \mathrm{RH}) - \arctan(\mathrm{RH} - 1.676331) + 0.00391838\mathrm{RH}^{1.5} \arctan(0.023101\mathrm{RH}) - 4.686035 \tag{2}$$

The assumption is that T_a and RH are consistent across construction sites. As a result, heat risk assessment varies depending on the value of T_g, which represents heat radiation. The microclimate simulation provides spatially-varying T_{mrt} values for the construction sites. These values are then transformed into T_g using Equation (3), derived from ISO 7726:

$$\mathrm{T_g}^4 - \mathrm{T_{mrt}}^4 + \frac{1.1 \times 10^8 \times \mathrm{V_a}^{0.6}}{\varepsilon \times \mathrm{D}^{0.4}} \times (\mathrm{T_g} - \mathrm{T_a}) = 0 \tag{3}$$

The globe emissivity (ε) is assumed to be 0.95, and the diameter of the globe thermometer (D) is 0.15m. To determine T_g, the quartic equation is solved under the assumption that the real number solution closest to both T_{mrt} and T_a is the value for T_g. Consequently, the outcome of this process is a WBGT-based heat risk map for the construction sites.

RISK-INFORMED DECISION-MAKING

The WBGT values serve as crucial information for identifying heat risks and implementing heat mitigation strategies. For instance, these values can be used to determine safety control thresholds. NIOSH offers recommended alert limits (RALs) and recommended exposure limits (RELs) in WBGT, Equation (4) and Equation (5), respectively:

$$\mathrm{RAL} = 59.9 - 14.1\ \log_{10} \mathrm{M} \quad (4)$$

$$\mathrm{REL} = 56.7 - 11.5\ \log_{10} \mathrm{M} \quad (5)$$

Where M is metabolic rate in Watts. For example, if M is 100 W, the WBGT of RAL is 31.7°C, and the WBGT of REL is 33.7°C. Additionally, NIOSH provides different RALs and RELs for short work periods and acclimatized workers, who may be able to withstand higher heat risks without experiencing adverse heat-related health effects (Jacklitsch et al. 2016). Furthermore, the WBGT information can be vital for planning heat mitigation strategies, as shown in Table 1 (adapted from the US Department of Defense). For instance, if the calculated WBGT value is 30°C, the recommended work/rest ratio for hard work is 30/30 minutes. Utilizing this information, heat mitigation strategies can be promptly developed by adjusting work schedules to effectively minimize heat exposure of construction workers.

Table 1. Recommendations for work/rest and water intake.

Heat Category	WBGT (°C)	Easy work (250 W)		Moderate work (425 W)		Hard work (600 W)	
		Work/Rest (min)	Water intake ($qt \cdot h^{-1}$)	Work/Rest (min)	Water intake ($qt \cdot h^{-1}$)	Work/Rest (min)	Water intake ($qt \cdot h^{-1}$)
1	25.6-27.8	Unlimited	0.5	Unlimited	0.75	40/20	0.75
2	27.8-29.4	Unlimited	0.5	50/10	0.75	30/30	1.0
3	29.4-31.1	Unlimited	0.75	40/20	0.75	30/30	1.0
4	31.1-32.2	Unlimited	0.75	30/30	0.75	20/40	1.0
5	32.2+	50/10	1.0	20/40	1.0	10/50	1.0

CASE STUDY ON SIMULATION-BASED HEAT RADIATION ASSESSMENT

A case study was conducted at the Architecture Quad on Texas A&M University Campus (30°37'05.8"N 96°20'14.3"W) on September 29, 2022, from 9:40 AM to 3:20 PM, to assess the accuracy of the microclimate simulation method. The performance of the simulation was compared using two on-site measurement techniques: (1) the six-directional method (Höppe 1992), which employed three net radiometers, and (2) the black globe thermometer method utilizing a globe thermometer sensor. Although the six-directional method is regarded as the most reliable measurement technique, its high cost and limited mobility pose significant limitations on its practical application. (Kántor et al. 2014). This study aims to compare the accuracy of the microclimate simulation-based method with both the six-directional method and the black globe thermometer method. Figure 4 illustrates the setup of the case study, featuring two weather stations: Station A, comprised of a globe thermometer sensor and two net radiometers, and Station B, a customized weather station with an additional net radiometer.

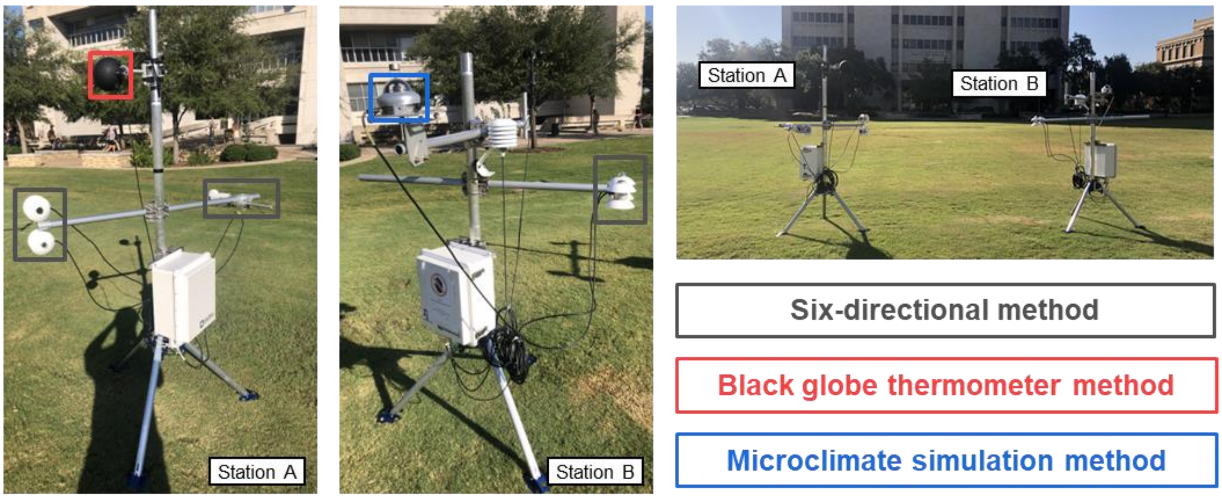

Figure 4. Experimental setups for the case study.

The collected meteorological data for the case study is shown in Figure 5. T_a steadily increased from 20.99°C to 29.8°C, while RH gradually decreased from 51.16% to 35.2%. The average GHI was 812.4 W/m², reaching a peak value of 923 W/m² at 13:50. Following its maximum, GHI decreased to 739.8 W/m² at 15:20, corresponding to the local standard time (LST). V_a was with a maximum of 6.65 m/s at 10:00 and then followed a decreasing trend. Figure 6 presents the outcomes of the case study comparing the six-directional method, the microclimate simulation method, and the black globe thermometer method. The microclimate simulation method demonstrates superior performance relative to the black globe thermometer method when compared to the six-directional method. The average difference for the black globe thermometer method is 11.17°C, with a maximum difference of 16.24°C. In contrast, the microclimate simulation method displays an average difference of -0.6°C and a maximum difference of 2.31°C. These findings align with previous research such as (Chen et al. 2014), which indicated a stronger correlation between the SOLWEIG results and the six-directional method than with the black globe method. The results of the black globe thermometer method exhibit more fluctuation than the other two methods. One potential explanation for this trend is the sensitivity of the equation from ISO 7726 to variations in V_a, as referenced by (Chen et al. 2014). Consequently, this also highlights the critical necessity of calibrating the black-globe thermometer method to accurately account for regional climatic conditions. This crucial aspect has been largely overlooked in previous construction-related research, leading to potential errors in the measurements.

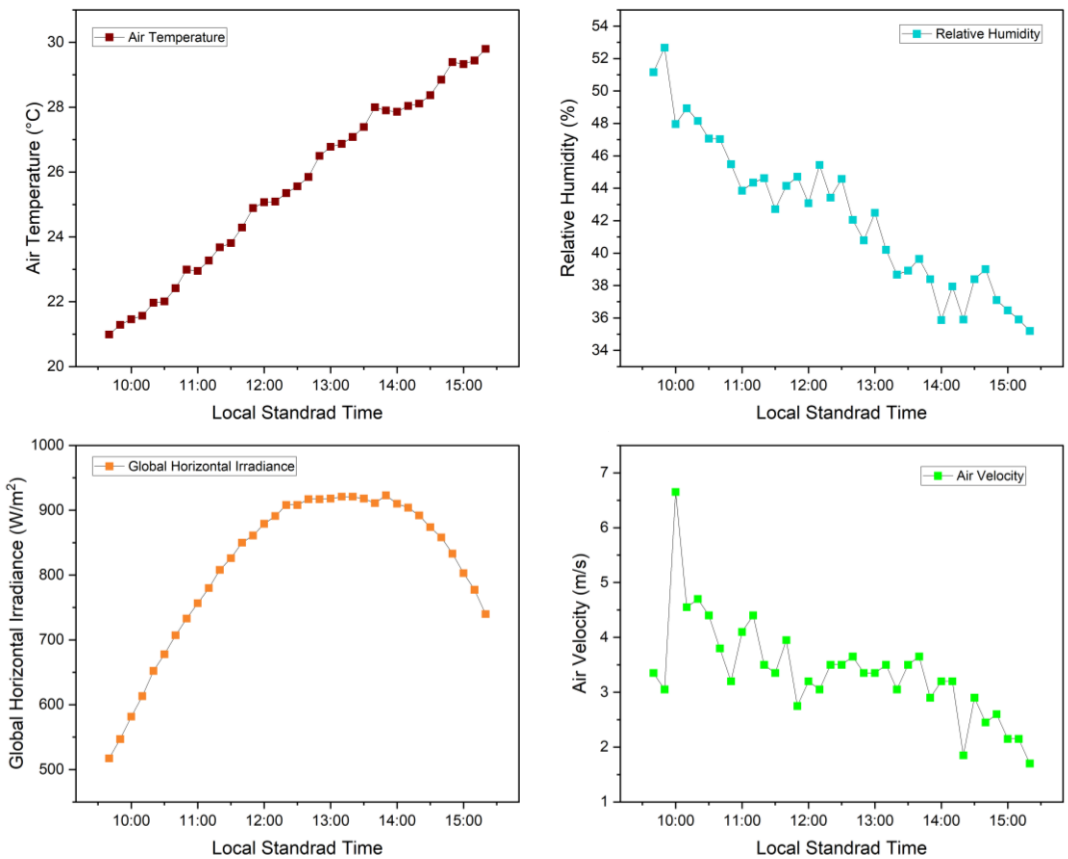

Figure 5. Meteorological conditions on 9/29/2022 (9:40~15:20).

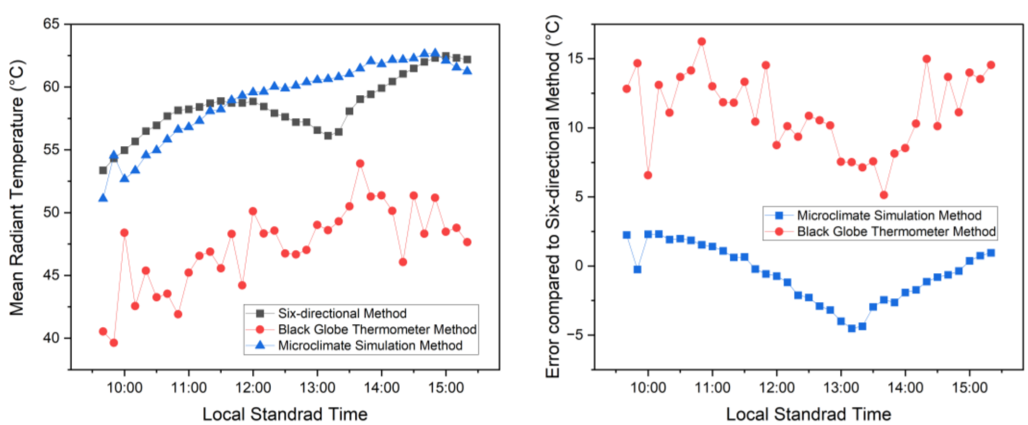

Figure 6. Comparison of results of the three methods and the errors compared to the six-directional method on 9/29/2022 (9:40~15:20).

CONCLUSION AND FUTURE WORKS

This study presents a novel heat stress monitoring framework that employs site modeling and microclimate simulation. A customized weather station transmits meteorological conditions to a server, enabling spatial heat risk assessments in a timely manner. Through a case study, the accuracy of the microclimate simulation method is validated in College Station, TX. Future research aims to implement this system on construction sites to explore the robustness of the proposed framework. By leveraging the benefits of understanding site-scale heat risks promptly, our research team is dedicated to developing a comprehensive solution that facilitates data-driven decision-making to protect the health and safety of construction workers. This aspect is currently being investigated as part of our ongoing research efforts.

ACKNOWLEDGEMENT

This material is in part based upon work supported by the National Science Foundation (NSF) under Award #2126045. Any opinions, findings, and conclusions or recommendations expressed in this material are those of the authors and do not necessarily reflect the views of the NSF.

REFERENCES

Chan, A. P. C., M. C. H. Yam, J. W. Y. Chung, and W. Yi. 2012. "Developing a heat stress model for construction workers." *Journal of Facilities Management*, 10 (1): 59–74.

Chen, Y.-C., T.-P. Lin, and A. Matzarakis. 2014. "Comparison of mean radiant temperature from field experiment and modelling: a case study in Freiburg, Germany." *Theor Appl Climatol*, 118 (3): 535–551.

Dong, X. S., G. H. West, A. Holloway-Beth, X. Wang, and R. K. Sokas. 2019. "Heat-related deaths among construction workers in the United States." *Am J Ind Med*, 62 (12): 1047–1057.

Fang, Z., T. Tang, Z. Zheng, X. Zhou, W. Liu, and Y. Zhang. 2021. "Thermal responses of workers during summer: An outdoor investigation of construction sites in South China." *Sustainable Cities and Society*, 66: 102705.

Gao, C., K. Kuklane, P.-O. Östergren, and T. Kjellstrom. 2018. "Occupational heat stress assessment and protective strategies in the context of climate change." *Int J Biometeorol*, 62 (3): 359–371.

Höppe, P. 1992. "A new procedure to determine the mean radiant temperature outdoors." *Wetter Leb*, 44: 147–151.

Jacklitsch, B., W. J. Williams, K. Musolin, A. Coca, J.-H. Kim, and N. Turner. 2016. *Occupational exposure to heat and hot environments*. Department of Health and Human Services, Centers for Disease Control and Prevention, Criteria for a Recommended Standard.

Jänicke, B., F. Meier, M.-T. Hoelscher, and D. Scherer. 2015. "Evaluating the Effects of Façade Greening on Human Bioclimate in a Complex Urban Environment." *Advances in Meteorology*, (T.-P. Lin, ed.), 2015: 747259. Hindawi Publishing Corporation.

Jones, B., G. Dunn, and D. Balk. 2021. "Extreme Heat Related Mortality: Spatial Patterns and Determinants in the United States, 1979–2011." *Spat Demogr*, 9 (1): 107–129.

Kamari, M., and Y. Ham. 2022. "AI-based risk assessment for construction site disaster preparedness through deep learning-based digital twinning." *Automation in Construction*, 134: 104091.

Kántor, N., C. V. Gál, Á. Gulyás, and J. Unger. 2018. "The Impact of Façade Orientation and Woody Vegetation on Summertime Heat Stress Patterns in a Central European Square: Comparison of Radiation Measurements and Simulations." *Advances in Meteorology*, (H. Tanaka, ed.), 2018: 2650642. Hindawi.

Kántor, N., T.-P. Lin, and A. Matzarakis. 2014. “Daytime relapse of the mean radiant temperature based on the six-directional method under unobstructed solar radiation.” *Int J Biometeorol*, 58 (7): 1615–1625.
Lin, R.-T., and C.-C. Chan. 2009. “Effects of heat on workers’ health and productivity in Taiwan.” *Global Health Action*, 2 (1): 2024.
Lindberg, F., and C. S. B. Grimmond. 2011. “The influence of vegetation and building morphology on shadow patterns and mean radiant temperatures in urban areas: model development and evaluation.” *Theor Appl Climatol*, 105 (3–4): 311–323.
Lindberg, F., S. Onomura, and C. S. B. Grimmond. 2016. “Influence of ground surface characteristics on the mean radiant temperature in urban areas.” *Int J Biometeorol*, 60 (9): 1439–1452.
Orlov, A., J. Sillmann, A. Aaheim, K. Aunan, and K. de Bruin. 2019. “Economic Losses of Heat-Induced Reductions in Outdoor Worker Productivity: a Case Study of Europe.” *EconDisCliCha*, 3 (3): 191–211.
Reja, V. K., K. Varghese, and Q. P. Ha. 2022. “Computer vision-based construction progress monitoring.” *Automation in Construction*, 138: 104245.
Stull, R. 2011. “Wet-Bulb Temperature from Relative Humidity and Air Temperature.” *Journal of Applied Meteorology and Climatology*, 50 (11): 2267–2269.
Tang, P., and Q. Li. 2022. “Evaluation of the observation methods of outdoor mean radiant temperature in a subtropical city.” *Building and Environment*, 207: 108462.
Wong, D. P., J. W. Chung, A. P. Chan, F. K. Wong, and W. Yi. 2014. “Comparing the physiological and perceptual responses of construction workers (bar benders and bar fixers) in a hot environment.” *Applied Ergonomics*, 45 (6): 1705–1711.
Yi, W., A. P. C. Chan, X. Wang, and J. Wang. 2016. “Development of an early-warning system for site work in hot and humid environments: A case study.” *Automation in Construction*, 62: 101–113.